Algorri, José Francisco, … et al. (2014). Generation of Optical Vortices by an Ideal Liquid Crystal Spiral Phase Plate. *IEEE Electron Device Letters*, 35(8), pp.: 856-858.

DOI: https://doi.org/10.1109/LED.2014.2331339

Generation of Optical Vortices by an Ideal Liquid Crystal Spiral Phase Plate

José Francisco Algorri, Virginia Urruchi, Braulio Garcia-Cámara, and José Manuel Sánchez-Pena, *Senior Member, IEEE*

***Abstract*— An ideal spiral phase plate based on liquid crystals and two high resistivity layers is proposed and theoretically analyzed. The proposed structure generates a spiral-like voltage with simple voltage control. The liquid crystal layer produces an optical phase shift that depends on the voltage distribution. These two effects cause light passing through the device to be twisted like a corkscrew around its travel axis. Because of the continuous phase shift, the proposed device is expected to exhibit a conversion efficiency of ∼100%. In addition, this device is more efficient and simpler than previously reported optical vortex generators. Moreover, the device is completely reconfigurable, i.e., the operating wavelengths and topological charges are tunable. The device can be used to reduce the fabrication costs of current devices and generate different orbital angular momentum modes with improved light efficiency, simplicity, and possibility of reconfiguration.**

***Index Terms*— Temperature sensors, thin film sensors, liquid crystals, microstructure.**

I. Introduction

OVER the last decade, helical wavefronts have been amongst the most extensively studied complex phase-shapes of light. Light beams with an azimuthal phase dependence of $\exp(-il\Phi)$, where l is the topological charge, have an orbital angular momentum associated with them, and when focused, they form rings instead of points in the focal plane. In recent years, the number of applications of this phenomenon has grown exponentially. It has been applied to beam shaping [1], optical tweezers [2], atom manipulation [3], free-space communication [4], and fiber optics communications with new types of fibers [5], among others. Optical vortices are usually generated using spiral phase plates (SPPs) [6] or computer generated holograms (CGHs) [7]. CGHs are created by digitally generating holographic interference patterns that are mathematically computed. Blazed forked gratings have been used to concentrate more energy in the first diffraction order [8]. Nonetheless, the fabrication of CGHs remains a difficult task. SPPs linearly vary the length of the optical path through an axially variable thickness. Owing to fabrication limitations, SPPs usually have discrete phase values. Another important disadvantage of SPPs is the absence of reconfigurability, which means that the topological charges and operating wavelengths are fixed. To solve this problem, spatial light modulators (SLM) have been proposed as alternatives to SPP [9]. This solution is not ideal because the SLM's characteristic structure, based on pixels surrounded by opaque areas, causes loss of light efficiency. Moreover, to separate the diffraction orders, the phase pattern should be combined with a blazed grating pattern. Recently, a novel device for generating a reconfigurable optical vortex has been proposed and demonstrated [10]. This device uses liquid crystal (LC) and pie slices of indium tin oxide (ITO) to generate quantized spiral phase steps. Although its reported efficiency is better than that of SLM (500 times greater diffraction efficiency), the device does not adhere to the concept of an ideal SPP as it generates quantized phase. Moreover, the fan out and the determination of the voltage required at each electrode complicates the use of the final device.

In this work, a novel structure having LC and high resistivity layers was proposed and theoretically studied. Earlier works have demonstrated the use of a high resistivity layer (modal control) for designing LC lenses [11], micro-axicon arrays [12] or arrays of optical elements [13]. The resistivity layer generates a spherical voltage distribution for certain values of the resistance and structural parameters. The proposed structure in this Letter can generate a continuous spiral phase profile, which is completely reconfigurable by using low voltages. This device is capable of generating several OAM modes. Its fabrication cost is low, and its application in optical tweezers or OAM mode division multiplexing would reduce complexity and improve efficiency, allowing transmissions over longer distances.

II. Structure and Operational Principle

The proposed device consists of two ITO coated substrates covered by a high resistivity layer. The substrates are separated by a spacer of thickness 20 μm. The resulting cavity is filled with a nematic LC. MDA-98-1602 from Merck was selected owing to its high birefringence. As this device is an adaptive phase-only modulator no twist of the molecules is necessary. For this reason, a homogenous alignment is required. One solution could be the use of a polyimide as alignment layer (e.g. PIA2000) rubbed in the direction of the electrodes for the upper glass and in the antiparallel direction for the other one. Figure 1(a) shows

Manuscript received April 19, 2014; revised June 9, 2014; accepted June 14, 2014. This work was supported by the Comunidad de Madrid under Grant FACTOTEM2 S2009/ESP-1781. The review of this letter was arranged by Editor C. Jagadish.

The authors are the Department of Electronic Technology, Carlos III University, Madrid E-28911, Spain (e-mail: jalgorri@ing.uc3m.es).

Color versions of one or more of the figures in this letter are available online at http://ieeexplore.ieee.org.

Digital Object Identifier 10.1109/LED.2014.2331339

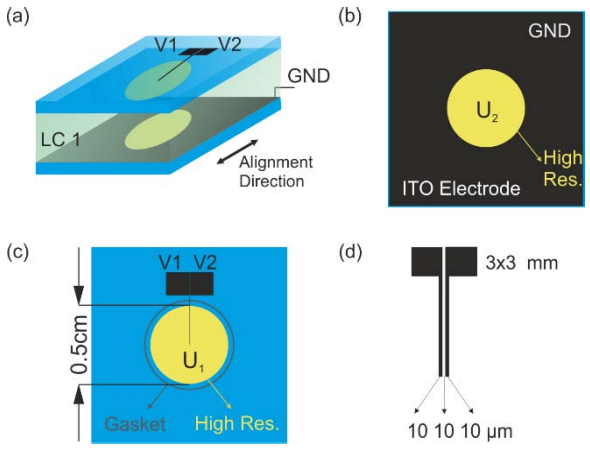

Fig. 1. Optical vortex generator. (a) Schematic of the device, (b) bottom substrate, (c) top substrate, and (d) electrode layout of the top substrate. Note: drawings are not to scale.

a schematic of the structure. The ground plane, shown in Fig. 1(b), includes a circular area without ITO at the center, which is covered with a high resistivity layer to generate a specifi voltage distribution (U_2). Figure 1(c) shows the upper plane composed of another circular area covered with a high resistivity layer. The voltage distribution in the upper plane is U_1. Additionally, this substrate includes two electrodes. The electrode pattern on the upper substrate consists of two striped ITO electrodes [Fig. 1(d)]. The substrates are arranged in such a manner that their circular areas are aligned with each other. Several materials can be employed, depending on the required sheet resistance (R_{sq}). For example, thin f lms of ITO, Nickel, Titanium Oxide (TiO_2), or PEDOT may be employed. The square resistance of these materials ranges from 0.1 to 10 MΩ/sq. In our structure, we considered a resistance of 0.1 MΩ/sq, voltage frequency of 1 kHz (in this case only one sinusoidal harmonic is considered), and thickness of 20 μm. In the following, V_1 and V_2 denote the applied voltage on the upper electrodes. The voltage distribution on the two high resistivity layers (U_1 and U_2) is described by the following second-order two-dimensional coupled partial differential equation (PDE) system,

$$\begin{cases} \nabla_s U_1^2 = R_{sq1}\,(G - j\omega C)\cdot(U_1 - U_2) \\ \nabla_s U_2^2 = R_{sq2}\,(G - j\omega C)\cdot(U_2 - U_1) \end{cases} \quad (1)$$

where U_1 and U_2 correspond to the voltage distribution in each high-resistivity layer, G and C refer to the conductance and capacitance across the LC layer, respectively, and R_{sq1} and R_{sq2} are the sheet resistances of the two high resistivity layers. In a previous work [13], the solution of this system was experimentally validated. We solved this problem numerically using the finit element method (FEM). Mixed boundary conditions, including Dirichlet (V_1, V_2 and ground voltage, GND) and Neumann boundary conditions, were used with a refi ed mesh. The theoretical analysis is made in the approximation of the constant boundary conditions at the electrodes. For the real case it would be necessary to bring the same voltage along the electrodes. In order to determine the LC molecular position (necessary to estimate the optical phase shift), we minimized the Gibbs free energy, F_G:

$$F_G = K_{11}\,(\nabla\vec{n})^2 + K_{22}\left(\vec{n}\cdot\nabla\times\vec{n} + \frac{2\pi}{\xi}\right) + K_{33}\,|\vec{n}\times\nabla\times\vec{n}|^2 - \frac{1}{2}\vec{D}\cdot\vec{E} \quad (2)$$

where $\vec{n}$ (n_x, n_y, n_z) represents the average local orientation of molecules, K_{ii}s are the elastic deformation constants, ξ is the pitch of a chiral helicoidal dopant (for twist purposes), D is the displacement vector, and E is the electric f eld. The solution of this equation, in combination with the solution of Eq. (1), yields the molecular distribution as a function of the applied voltages (V_1, V_2). Because the molecular position also affects the voltage distribution, an iterative process is necessary to determine both the f nal voltage and molecular position. The molecular distribution generates a gradient in the refractive index of the LC, which is proportional to the voltage. We estimate the phase shift by using the Fresnel approximation [14]. For the simulations, we extracted all the parameters from the datasheet, and these are listed in Table I.

TABLE I
MDA-98-1602 NEMATIC LC CHARACTERISTICS

Elastic Constants	Birefringence	Permittivity
K_{11}=15.7 pN	n_e=1.7779	ε_e=16.2
K_{22}=8 pN	n_o=1.5113	ε_o=12
K_{33}=13.6 pN	Δn=0.2666	Δε=4.3

III. RESULTS AND DISCUSSION

The simulation indicates the amplitude of voltage required to generate specif c OAM modes. We believe that the proposed simulation tool will be advantageous in estimating the voltages to be applied. Figure 2 shows the results of the simulation. These results were obtained by estimating the voltage distribution and molecular orientation of LC molecules in the active area. As shown, the applied voltages V_1 and V_2 are 1.2 V_{rms} and 2.5 V_{rms}, respectively, in Figs. 2(a), (c) and 2.5 $_{rms}$ and 1.2 V_{rms}, respectively, in Figs. 2(b), (d). The LC layer can produce eight different OAM modes; $l = \pm1, \pm2, \pm3$, and ±4, where l is the topological charge determined by the number of phase changes per wavelength around the beam axis. In Fig. 2 we considered topological charges of $l = 4$ and $l = -4$. We found that small changes in the applied voltage result in large changes in phase shift. Note that multiples of 2π are needed to create optical vortices. Further, with slight changes of the applied voltage, the phase shift can be maintained at 2π (or its multiple), but the operation wavelength changes.

Another advantage of the device is the generation of several topological charges. The point spread function (PSF) of an optical vortex provides information about its topological charge. The PSF is the impulse response of a focused optical system, i.e., it shows the distribution of the light intensity of the focal spot. Figure 3 displays the PSF for several voltages for $\lambda = 632.8$ nm and pupil diameter = 5 mm, evaluated by considering the optical path length and using Fourier transforms.

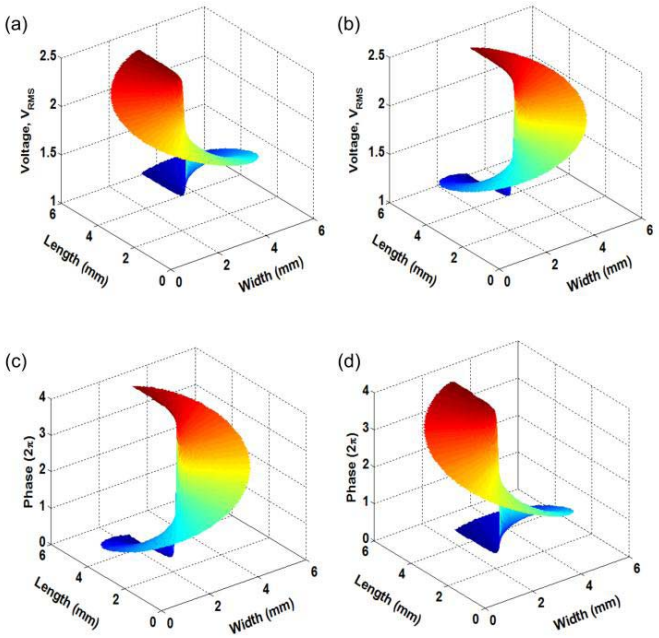

Fig. 2. Simulated results of the voltages seen by the LC (upper part) and the 3D phase shift (bottom part) when the voltages applied to the ITO electrodes are $V_1 = 1.2$ Vrms and $V_2 = 2.5$ Vrms [(a) and (c)] 3D or $V_1 = 2.5$ Vrms and V2 = 1.2 Vrms [(b) and (d)].

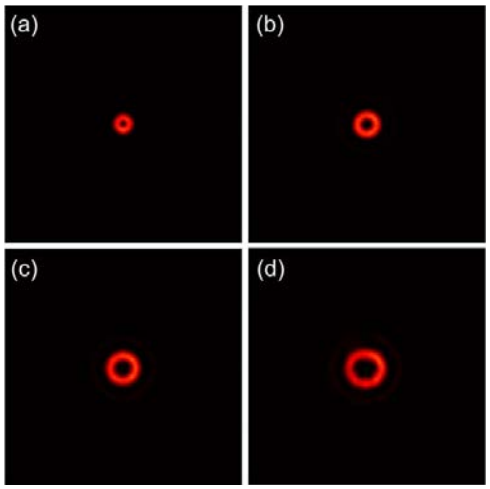

Fig. 3. Tunable topological charge for (a) $V_1 = 1.2$ Vrms and $V_2 = 1.5$ Vrms, (b) $V_1 = 1.2$ Vrms and $V_2 = 1.8$ Vrms, (c) $V_1 = 1.2$ Vrms and $V_2 = 2.1$ Vrms, and (d) V1 = 1.2 Vrms and V2 = 2.5 Vrms.

These results demonstrate that the topological charge can be controlled with precision. A slight variation of V_2 allows four different modes to be achieved. The negative topological charge can be easily determined by interchanging the voltages at V_1 and V_2, as shown in Fig. 2. There are two characteristic curves in the LC birefringence response as a function of voltage that have to be avoided. The first one is produced when the electrical energy overcomes the elastic free energy and the molecules start to move. The other one is produced when the molecules start to reach the perpendicular position. In this case, the cuasi-linear range between this curves ranges from 1.2 Vrms to 2.5 Vrms. As an ideal SPP is characterized by a linear phase drop, this operating range has to be mantained. For example, above 2.5 V_{rms}, the relation between voltage and phase shift is non-linear, resulting in a non-perfect, spiral-like phase. By increasing the device thickness, more topological charges can be easily generated. For instance, a thickness of 40 μm yields 8 positive and negative topological charges.

IV. Conclusion

In summary, a novel optical vortex generator was proposed and theoretically analyzed. Simulations reveal that small changes in the applied voltage produce large changes in the phase shift. We conclude that simulations are essential for using this device because important design parameters, such as the thickness, square resistance of the deposited layer, and the frequency and amplitude of the voltage control, can be optimized prior to application. Owing to the continuous optical phase shift, this device is the best approximation to an ideal SPP proposed to date. Moreover, the device is completely reconfigurable (operating wavelengths and topological charges are tunable). The device can be used in new applications (e.g. fiber optics communications or atom manipulation), to reduce the fabrication costs of existing devices, and to generate different OAM modes with improved light efficiency, simplicity, and possibility of reconfiguration.

References

[1] M. Padgett and R. Bowman, "Tweezers with a twist," *Nature Photon.*, vol. 5, no. 6, pp. 343–348, May 2011.
[2] K. Ladavac and D. G. Grier, "Microoptomechanical pumps assembled and driven by holographic optical vortex arrays," *Opt. Exp.*, vol. 12, no. 6, pp. 1144–1149, 2004.
[3] J. W. R. Tabosa and D. V. Petrov, "Optical pumping of orbital angular momentum of light in cold cesium atoms," *Phys. Rev. Lett.*, vol. 83, pp. 4967–4970, Dec. 1999.
[4] J. Wang *et al.*, "Terabit free-space data transmission employing orbital angular momentum multiplexing," *Nature Photon.*, vol. 6, no. 7, pp. 488–496, Jun. 2012.
[5] N. Bozinovic *et al.*, "Terabit-scale orbital angular momentum mode division multiplexing in fibers," *Science*, vol. 340, no. 6140, pp. 1545–1548, 2013.
[6] M. W. Beijersbergen *et al.*, "Helical-wavefront laser beams produced with a spiral phaseplate," *Opt. Commun.*, vol. 112, no. 6, pp. 321–327, 1994.
[7] N. R. Heckenberg *et al.*, "Generation of optical phase singularities by computer-generated holograms," *Opt. Lett.*, vol. 17, no. 3, pp. 221–223, 1992.
[8] I. Zeylikovich *et al.*, "Ultrashort Laguerre–Gaussian pulses with angular and group velocity dispersion compensation," *Opt. Lett.*, vol. 32, no. 14, pp. 2025–2027, 2007.
[9] K. Crabtree, J. A. Davis, and I. Moreno, "Optical processing with vortex-producing lenses," *Appl. Opt.*, vol. 43, no. 6, pp. 1360–1367, 2004.
[10] J. Albero *et al.*, "Liquid crystal devices for the reconfigurabl generation of optical vortices," *J. Lightw. Technol.*, vol. 30, no. 18, pp. 3055–3060, Sep. 15, 2012.
[11] G. D. Love and A. F. Naumov, "Modal liquid crystal lenses," *Liquid Crystals Today*, vol. 10, no. 13, pp. 1–4, 2000.
[12] J. F. Algorri, G. D. Love, and V. Urruchi, "Modal liquid crystal array of optical elements," *Opt. Exp.*, vol. 21, no. 21, pp. 24809–24818, 2013.
[13] J. F. Algorri *et al.*, "Modal liquid crystal microaxicon array," *Opt. Lett.*, vol. 39, no. 12, pp. 3476–3479, 2014.
[14] J. W. Goodman, *Introduction to Fourier Optics*. New York, NY, USA: McGraw-Hill, 1968.